

1 TITLE

2 PRE-BORDER GENE FOXB1 REGULATES THE DIFFERENTIATION TIMING
3 AND AUTONOMIC NEURONAL POTENTIAL OF HUMAN NEURAL CREST
4 CELLS

5

6 AUTHORS

7 Alan W. Leung^{1*#}, Francesc López-Giráldez², Cayla Broton¹, Kaixuan Lin¹, Maneeshi S.
8 Prasad³, Jacqueline C. Hernández³, Andrew Z. Xiao^{1*}, Martín I. Garcia-Castro^{3*}

9

10 AFFILIATIONS

11 ¹Department of Genetics and Yale Stem Cell Center, Yale School of Medicine, New
12 Haven, CT 06520, USA

13 ²Yale Center for Genome Analysis, Yale University School of Medicine, New Haven, CT
14 06520, USA

15 ³School of Medicine Division of Biomedical Sciences, University of California,
16 Riverside, CA 92521, USA

17

18 *Correspondence

19 A.W.L. - leungwailun@gmail.com

20 A.Z.X. - andrew.xiao@yale.edu

21 M.I.G.C. - martin.garcia-castro@ucr.edu

22

23 #Lead contact

24 A.W.L.

25 SUMMARY

26 What are the factors that are induced during the transitory phases from pluripotent stem
27 cells to lineage specified cells, how are they regulated, and what are their functional
28 contributions are fundamental questions for basic developmental biology and clinical
29 research. Here, we uncover a set of pre-border (pB) gene candidates, including forkhead
30 box B1 (FOXB1), induced during human neural crest (NC) cell development. We
31 characterize their associated enhancers that are bound by pluripotency factors and rapidly
32 activated by β -catenin-mediated signaling during differentiation. Surprisingly, the
33 endogenous transient expression of FOXB1 directly regulates multiple early NC and
34 neural progenitor loci including *PAX7*, *MSX2*, *SOX1*, and *ASCL1*, controls the timing of
35 NC fate acquisition, and differentially activates autonomic neurogenic versus
36 mesenchymal fates in mature NC cells. Our findings provide further insight into the
37 concept of the less characterized pB state and clearly establishes FOXB1 as a key
38 regulator in early cell fate decisions during human pluripotent stem cell differentiation.

39 **KEYWORDS**

40 Differentiation; Pluripotent Stem Cells; Human Development; Forkhead box B1;

41 Transcription Factors; Neural border; Neural Crest; Autonomic Neurons

42 INTRODUCTION

43 A fundamental question in developmental biology is how pluripotent cells transit
44 from pluripotency towards lineage specification (Kalkan and Smith, 2014). Recent advent
45 of time-series single cell RNA-sequencing has revealed dynamic transcriptional features
46 and cell states during pluripotent cell differentiation *in vivo* and *in vitro* (Pijuan-Sala et
47 al., 2018). Gain of function by overexpression, and loss or reduction of function
48 (knockdown and knockout) approaches, such as CRISPR/CRISPR
49 interference/siRNA/miRNA screening and reporter assays, have also been used to
50 identify genes that are important for initial cell fate decision from pluripotent cells
51 (Arduini and Brivanlou, 2012; Betschinger et al., 2013; Genga et al., 2019; Hackett et al.,
52 2018; Ma et al., 2015; Wang et al., 2012). To functionally characterize novel cell states,
53 there is an urgency to develop experimental pipelines that will integrate the various
54 molecular inputs, effectors, and feedback regulations to infer an increasingly
55 sophisticated road map of cellular differentiation.

56 Neural crest (NC) is an embryonic cell population that emerges from the dorsal
57 neural tube, migrates extensively, and generates peripheral nervous system neurons and
58 glia, and ectomesenchyme-derived craniofacial bone and cartilage, amongst many other
59 derivatives (Prasad et al., 2019; Stuhlmiller and Garcia-Castro, 2012). This wide range of
60 differentiation potential defies canons of sequential segregation of potential because NC
61 has been considered to emerge from the ectoderm, and bone and cartilage derivatives are
62 normally only associated with mesoderm, not with ectoderm. This issue remains
63 unresolved, with a general perception that the ectodermally-restricted NC lineage
64 acquires ectomesenchymal capacity. Hall suggested that NC constituted a fourth germ
65 layer, but provided little mechanistic evidence (Hall, 2000). Work in chick and rabbit
66 embryos has challenged the classic perception of NC ontogeny, postulating that the early,
67 and thus anterior NC, are specified during gastrulation, independently of mesoderm and
68 or neural interactions and thus postulating a pre-germ layer origin (Basch et al., 2006;
69 Betters et al., 2018). Our unpublished work has further identified in chick blastula
70 embryos with matching experiments in human embryonic stem (ES) cells a NC
71 specification status in pre-streak epiblast within chick embryos and within hours after
72 initiation of NC induction from human ES cells that is distinct molecularly and

73 functionally from pluripotent stem cells (Prasad et al 2019, submitted).

74 Previously we established a robust model in human pluripotent stem cells, which
75 produce NC cells with anterior character, and allowed us to interrogate the ontogeny of
76 human anterior NC (Leung et al., 2016). In this process of NC induction, we uncovered a
77 class of genes, which we dubbed as pre-border (pB) genes (including *GBX2*, *SP5*, *ZIC3*
78 and *ZEB2*) that are induced prior to, and with distinct signaling requirements than, classic
79 neural plate border genes (Leung et al., 2016). The biological significance of these pB
80 genes is currently not clear. Evidence from vertebrate embryos and cell reprogramming
81 supports the existence of a ‘pB-like’ cell state prior to the emergence of neural border or
82 definitive neurectoderm (Basch et al., 2006; Betters et al., 2018; Thier et al., 2019;
83 Trevers et al., 2018). The concept of pB cell state however is poorly characterized. In our
84 previous study, we proposed the idea that NC specification takes place prior and
85 independently of neurectoderm commitment (Leung et al., 2016). Here we aim to
86 scrutinize the transcriptome and dissect the molecular functions of pB candidate genes
87 and aim to provide further insights into the earliest lineage specification events during the
88 exit of pluripotency towards NC lineage.

89 Forkhead box (FOX) family proteins are important factors in disease and
90 development (Golson and Kaestner, 2016). They contain a DNA binding domain known
91 as a forkhead or wing helix domain and these proteins can act either as pioneer factors to
92 open local chromatin structures, as classic transcription factors, or both (Iwafuchi-Doi
93 and Zaret, 2016; Lalmansingh et al., 2012). They play essential roles in the regulation of
94 mammalian pluripotency (Krishnakumar et al., 2016; Respuela et al., 2016) and in the
95 specification and further differentiation of neural crest (Kos et al., 2001; Lukoseviciute et
96 al., 2018; Sasai et al., 2001; Seo et al., 2017; Seo and Kume, 2006; Teng et al., 2008; Xu
97 et al., 2018).

98 *Foxb1* is strongly expressed in epiblast, neural plate, neuroepithelium, and
99 midbrain neural folds including NC progenitors (Labosky et al., 1997). Lineage tracing in
100 mice suggests contributions to multiple lineages, including NC derivatives (Zhao et al.,
101 2007). *Foxb1*^{-/-} mice displayed developmental delay, posterior truncation, and open
102 neural tube phenotype (Labosky et al., 1997). These mice also lacked a subgroup of
103 medial mammillary body neurons implicated in spatial memory and behaviors (Wehr et

104 al., 1997). Foxb1 could act as a survival factor for these mammillary neurons during the
105 formation of mammillo-thalamic axonal tract (Alvarez-Bolado et al., 2000). In frog
106 embryos, forced expression of Foxb1 led to increased neural induction mediated via
107 cooperation with a Pou transcription factor (Takebayashi-Suzuki et al., 2011) It is of note
108 that a human patient with intellectual disability and distinctive facial features was found
109 with large 15q22.2 deletion spanning the *FOXB1* locus (Yamamoto et al., 2014). The
110 function of FOXB1 during human ES differentiation is currently unknown.

111 In this work, by studying the transcriptomic changes, enhancer utility, molecular
112 functions, and genomic binding patterns of pB candidates, we aim to reveal the
113 importance of pB intermediate during the exit of pluripotency and the specification of NC
114 cells. Our data uncovers 68 candidates for pB intermediate and reveals that these gene
115 candidates are regulated by elements pre-occupied by pluripotency factors and β -catenin
116 co-factors. Our data also reveals major functions of FOXB1, a key pB candidate, in
117 controlling the timing of NC differentiation, and regulating the differentiation potential of
118 NC precursors towards autonomic neuronal fates. Finally, we provide genomic-binding
119 data of FOXB1 showing that these functions are carried out by direct transcriptional
120 controls on key neurogenic and NC gene loci. Altogether, our data provides important
121 new insights into the poorly characterized pB cellular state and reveals FOXB1 as an
122 essential regulator of human ES cell differentiation. Our data further highlights the
123 critical function of FOXB1 in conferring autonomic neurogenic potential to pre-NC cells.
124

125 RESULTS

126 ES cell transcriptional response to canonical WNT signaling during NC induction

127 Human NC cell induction using our established protocol takes 5 days (Leung et
128 al., 2016) and progresses via a pB and a neural border stage (Fig. 1A) to generate
129 SOX10⁺ NC cells that do not express the definitive neurectoderm marker PAX6 along
130 their course of induction (Fig. 1B) (Leung et al., 2016). To trace the transcriptomic
131 trajectory of early human NC progenitors, we performed time-course mRNA sequencing
132 (RNA-seq) of human ES cells, cells derived from differentiation day 3 (pre-NC,
133 representing a mixture of pB and neural border progenitors) and differentiation day 5
134 (representing NC progenitors). RNA-seq samples were classified by unsupervised
135 hierarchical clustering according to their differentiation status (Fig. 1C). Differential
136 expression ($p < 0.05$) was respectively detected at 3338 (ES cells versus day 3), 4424 (ES
137 cells versus day 5) and 2009 (day 3 versus day 5) loci. The RPKM values and fold
138 changes comparing different time points for all mapped transcripts are provided in table
139 S1. Factors known to regulate pluripotency and self-renewal including *POU5F1* and
140 *NANOG*, except *SOX2*, and components for FGF (*FGF2*, *DUSP6*), and NODAL
141 (*NODAL*, *GDF3*, *LEFTY1*, *LEFTY2*, *TDGF1*) signaling were downregulated during
142 differentiation (Fig. 1D). Previously identified pB transcripts *GBX2*, *ZIC3*, *ZEB2*, and
143 *SP5*, as well as *MEIS2* (a known NC factor), were dramatically upregulated at day 3 (Fig.
144 1E). This was followed by a gradual induction of neural border and NC transcripts
145 including *PAX3*, *PAX7*, *TFAP2A*, *NR2F1*, *MSX1*, *MSX2*, *SNAI2*, *NR2F1*, *CDH6*, *SOX9*
146 and *SOX10*, while *FOXD3* and *ETS1*, displayed a biphasic expression pattern (Fig. 1D,
147 E). As expected for their essential roles in human NC cell induction (Leung et al., 2016),
148 ligands for WNT and BMP pathways, as well as their receptors (*FZDs*) and extracellular
149 regulators (*CHRD*, *NOG*, *BMPER*), were upregulated synchronously during
150 differentiation (Fig. S1A). Signaling components for Hedgehog (*HHIP*, *GLII*, *GLI3*,
151 *SMO*, *SUFU*), NOTCH (*JAG1*, *HES3/4*), and insulin growth factor (IGF) (*IGF1*, *IGF1R*,
152 *IGFBP2/5* and *PAPPA*) pathways were either induced or repressed with their general
153 trends indicative of either a blockade (Hedgehog) or activation (Notch and IGF) of the
154 pathways (Fig. S1B). Notably, increased transcription of imprinting loci *IGF2* and *H19*
155 was observed at both day 3 and day 5 (Fig. S1C). Few selected *HOX* genes, except

156 *HOXA1* and *HOXB1/2* (Fig. S1C), were activated, suggestive of cranial character of our
157 NC progenitors.

158 To systematically identify a complete pB gene set, we subjected day 3
159 transcriptome data to further analyses based on p values (<0.05), RPKM values (>8.2,
160 expressing at a higher absolute transcript level than *GBX2*, a known pB gene), and fold
161 changes (>10 folds over ES cells) of individual transcripts (Fig. 1F). Based on these
162 criteria, 68 transcripts were identified (Fig. 1F'). These transcripts were expressed and
163 induced at much higher level than neural border and NC transcripts. To examine the cell
164 type specificity of these pB candidates, we performed RT-qPCR on 4 cell types: ES cells,
165 pre-NC, prospective anterior neuroectoderm (NE) and non-neural ectoderm (NNE) (Fig.
166 S1D). We found that 45.6% (n=31/68) and 19.1% (n=13/68) of pB candidates were “NC-
167 specific” (Fig S1E) and “NC-enriched” (Fig S1F) respectively and were expressed at
168 significantly higher levels in pre-NC cultures than those under ES cells, NE or NNE
169 condition. For “NC-specific” pB candidates, no significant transcriptional induction was
170 detected under NE and NNE conditions compared to ES (Fig S1E). These two categories
171 together constitute 64.7% of all pB candidates. The rest of the candidates were either
172 “NC-biased” (n=7/68, Fig S1G, induced under NC condition but no consistent increase in
173 expression was observed compared NC versus NNE and NE), assuming a “broad
174 ectoderm expression” pattern (n=7/68, Fig S1H, significant induction detected in all 3
175 ectoderm lineages), or “highly variable in expression or not specific to NC” (n=10/68,
176 Fig S1I, no significant induction detected under NC condition). In conclusion,
177 transcription of a majority of pB candidates was highly specific and enriched in early NC
178 cultures.

179

180 β -catenin dependent activation of early NC response genes

181 pB genes including *GBX2*, *ZEB2*, *ZIC3*, and *SP5* were known to be regulated by
182 β -catenin (CTNNB1) signaling (Leung et al., 2016). As expected, β -catenin was the top
183 predicted upstream regulator for differentially expressed genes found in our
184 transcriptome (p=4.6e-27 and 1.36e-27 for day 3 and day 5 transcriptomes respectively,
185 Fig. S2A). To test if pB candidates were β -catenin transcriptional targets, we examined
186 the expression of 12 selected pB candidates, identified above as showing “NC-specific”

187 induction (Fig S1E), in ES and differentiating cells that were transduced with either a
188 *luciferase* shRNA or a β -*catenin* shRNA (Fig 2A). First we found that β -*catenin* shRNA
189 downregulated β -*catenin* (*CTNNB1*) RNA expression at ES and day 1, but did not affect
190 expression of pluripotency factor *POU5F1* (Fig. 2B). At day 1, a majority of pB
191 candidates (7 out of 12) however were repressed by β -*catenin* shRNA (Fig. S2B).
192 Notably, no change in pB candidate expression was detected in β -*catenin* shRNA cell
193 line. By day 3, all 12 pB candidates were downregulated in β -*catenin* shRNA-transduced
194 cultures (Fig. S2C). To confirm the expression dynamics of the rest of the pB candidates,
195 we performed RNA-seq on cultures transduced with control *luciferase* or β -*catenin*
196 shRNAs derived from ES cells, at day 1 and at day 3 (Fig. 2C, table S2). In line with our
197 earlier time-course transcriptome analysis, 95.6% pB candidates (n=65/68) were induced
198 in control *luciferase* shRNA cultures at day 3. Out of these candidates, 73.8% (n=48/65)
199 displayed a 2-fold or more downregulation in β -*Catenin* shRNA cultures. A lower, yet
200 significant, proportion of pB candidates (44.1%, n=30/68) were already induced in
201 control day 1 cultures. Almost all of them (96.7%, n=29/30) were downregulated in β -
202 *catenin* shRNA-transduced cultures.

203 FGF and BMP signaling are known to promote NC induction. To test if these
204 signaling pathways contributed to the induction of pB candidates, we activated these
205 pathways under NC condition using FGF2 (Fig. 2D) or BMP4 (Fig. 2E) ligand. Out of
206 the 12 “NC-specific” pB candidates we tested, a majority of them were repressed to basal
207 transcriptional level by either of these ligands suggesting that high FGF or BMP
208 signaling did not favor pB candidate induction from ES cell cultures.

209 Altogether, these data establishes canonical WNT signaling is the main
210 contributor among major signaling pathways for pB candidate induction (Fig. 2F) and β -
211 *catenin* is a positive regulator for pB candidate induction during NC induction.

212

213 Early NC response genes are Poised for Transcriptional Activation in Pluripotent Stem 214 Cells

215 Expression of many pB candidates were robustly induced within 24 hours from
216 the start of differentiation (Fig. S1C, E). It is possible that pluripotency factors expressed
217 in ES cells might prime developmental genes such as pB candidates for which a rapid β -

218 catenin activation was found.

219 By visual inspection of published ChIP-seq datasets for key pluripotency factors
220 (NANOG, POU5F1, SOX2, BCL11A)(Gertz et al., 2013; Tsankov et al., 2015), β -
221 catenin cofactors (NIPBL, LEF1, TCF4)(Estaras et al., 2015; Tsankov et al., 2015), and
222 chromatin signature marks (Consortium, 2012; Rada-Iglesias et al., 2011), we identified
223 putative regulatory elements close to pB candidate genes *GBX2* (Fig. S3A) and *FOXB1*
224 (Fig. S3B). These 2 elements displayed strong binding of pluripotency factors and β -
225 catenin co-factors, open chromatin configuration (ATAC-seq), presence of enhancer
226 marks (EP300, H3K4me1), and β -catenin (CTNNB1) binding upon CHIR 99021(Funa et
227 al., 2015) or WNT ligand (Estaras et al., 2015)-mediated ES cell differentiation. To
228 identify other putative pB candidate regulatory elements, we tested the co-occupancy of
229 pluripotency factors and β -catenin cofactors by performing pairwise comparisons of the
230 ChIP-seq peak sets for pluripotency factors and β -catenin cofactors (Fig. S3C). We found
231 significant overlaps for all pairwise comparisons ($p < 10^{-4}$) (Fig. S3C, Table S3). Among
232 these comparisons, NANOG and NIPBL had the largest overlapping binding regions
233 ($n=37,481$, Fig. S3E). Notably, these NANOG-NIPBL co-bound elements with
234 characteristics of poised or inactive enhancers (Fig. S3F) were significantly associated
235 with developmental processes for NC cells (NC differentiation/development, PNS
236 development, abnormal craniofacial morphology) and gene expression in ectoderm
237 (TS11/12/14 embryonic ectoderm) (Fig. S3G). These poised and inactive enhancers were
238 also represented in high percentage ($>50\%$) within the 199 NANOG-NIPBL co-bound
239 elements associated with the 68 pB candidate loci (Fig. S3H). Among these 199 pB
240 associated NANOG-NIPBL co-bound elements, a high percentage was also bound by β -
241 catenin upon canonical WNT-mediated differentiation. Such elements were found at
242 genomic location upstream (Fig 3A), downstream (Fig 3B), or within intronic sequences
243 (Fig 3C) of pB candidate loci. To conclude, these *in silico* analysis supports the model
244 that β -catenin signaling during NC induction unlocks poised or inactive enhancers for pB
245 genes thereby leading to their increased transcription.

246 To confirm the above *in silico* analysis that NANOG pre-occupied pB candidate
247 regulatory elements and to visualize NANOG binding dynamics during NC induction, we
248 performed NANOG CHIP-qPCR on ES and differentiation day 3 cells. We confirmed

249 that 76.9% of all elements tested (n=10/13) have enriched NANOG binding at human ES
250 cell stage. NANOG is known to prime developmental gene loci. During ES cell
251 differentiation, NANOG is also known to repress NC gene transcription (Wang et al.,
252 2012). While a smaller subset (n=6/13) still had significant NANOG binding at day 3,
253 NANOG binding was much attenuated at day 3 as we detected an overall decreasing
254 trend of NANOG binding in 53.8% of tested elements (n=7/13) at day 3 as compared to
255 day 0 (Fig. 3D).

256 To demonstrate these enhancers were activated upon NC induction, ChIP-qPCR
257 analysis the enhancer mark H3K27ac was carried on pB candidate regulatory elements in
258 human ES cells (day 0) and differentiation day 3 cells. The data revealed that a majority
259 of (76.9%, n=10/13) of the tested elements displayed increased accumulation of
260 H3K27ac mark (Fig. 3C), demonstrating that these elements became more active during
261 differentiation.

262 Lastly, to functionally test these pB enhancer elements, we used CRISPR
263 approach to knock out one of them, the FOXB1-E1 (asterisk, Fig. 3B and 3E), a
264 NANOG-NIPBL co-bound and β -catenin bound element that resides immediately
265 upstream of the *FOXB1* gene. Deletion of this 495-bp E1 element (top panel, Fig. 3F) led
266 to reduction of *FOXB1* transcription in differentiating cells in a day wise time course
267 experiment (Fig. 3G). Further differentiation assay with additional knockout cell lines
268 (FOXB1-E1-KO1, -KO2, -KO3) confirmed the time course experimental result in that
269 removal of FOXB1-E1 element led to significantly reduced transcription of FOXB1 gene
270 at differentiation day 1 (47%±30% of control level, p<0.01), day 3 (30%±14% of control
271 level, p<0.001), and day 5 (21%±11% of control level, p<0.01) (Fig. 3H). The
272 downregulation of *FOXB1* in differentiating cells strongly indicated that *E1* element
273 acted as a functional enhancer for FOXB1 induction and its continued expression. These
274 data together suggest that distinct regulatory elements primed by NANOG and NIPBL,
275 and bound by β -catenin during early differentiation of human ES cells positively
276 regulated pB candidate transcription.

277

278 Pre-Border Candidates are expressed in chick epiblast prior to overt neural plate border
279 formation

280 As a first approach to decipher the function of pB genes, we focus on *FOXB1*
281 which has a known role in lineage differentiation. Our RNA-seq data suggests that it is
282 expressed at high level at differentiation day 3 during NC induction but not at ES cells or
283 day 5 cultures (Fig 4A, S4A). This result is consistent with lineage tracing of *Foxb1* in
284 murine embryos revealing its expression in NC precursors but not in mature NC cells or
285 their derivatives (Zhao et al., 2007). By RT-PCR we confirmed that during human NC
286 induction *FOXB1* was transiently induced and peaked at day 2 or day 3 similar to other
287 documented pB genes (Leung et al., 2016), and its expression complemented two highly
288 expressing FOX factors, *FOXD3* and *FOXH1*, which either rapidly downregulated upon
289 differentiation (*FOXH1*) or assumed a bi-phasic expression pattern (*FOXD3*) (Fig. 3G,
290 4B). Whereas most other FOX factors *FOXA3*, *FOXI3*, *FOXN3*, and *FOXO4* showed
291 decreased expression in day 3 compared to ESC, the only two other FOX factors that
292 showed increased transcription at day 3 were *FOXOB3* and *FOXP4* but their fold
293 increase in RPKM was limited to around 2 fold compared to more than 10 fold for
294 *FOXB1*. In agreement to transcript analysis, *FOXB1* protein was detected at day 3, but
295 not in human ES cells (Fig. S4B). We reasoned that *FOXB1* carried a unique function
296 during the early differentiation window, when other FOX factors were not as highly
297 expressed.

298 Expression of *Foxb1* is first detected in gastrulating mouse embryos in the
299 primitive streak and the surrounding epiblast (Labosky et al., 1997). In chick
300 embryos, *Foxb1* was expressed at the same location at Hamburger-Hamilton (HH) stage
301 4 (Fig. 4C), posterior to the caudal boundary of the anterior neural marker *Ganf*
302 (Fernandez-Garre et al., 2002), and just before *Pax7* induction at the prospective neural
303 border at HH4+ (Basch et al., 2006). *In situ* hybridization for other pB candidates with
304 chicken homologs including *Cntn2*, *Prmt8*, *Nrcam*, *Plagl1*, *Stmn2*, *Enpp2*, and *Enc1*
305 showed similar expression patterns as *Foxb1* at HH stage 4 (n=7, Fig. S4C). Notably,
306 *Foxb1* robust expression is restricted to the ectoderm/epiblast layer (arrows, Fig. 4C').
307 Upon development, *Foxb1* expression progressively restricted medially as neural plate
308 developed (Fig. 4D), and was visibly extinct from the neural border at HH8
309 (asterisks, Fig 4D'). The broad expression domain of *Foxb1* in early epiblast cells could

310 represent a competent zone for NC development, and hinted at a function for Foxb1 in
311 prospective NC populations prior to the formation of the neural border.

312

313 Loss of FOXB1 De-Repressed Neural Crest Development

314 To interrogate the function of FOXB1 in human ES cell differentiation, we
315 attempted to reduce expression level of FOXB1 induced by administration of a *FOXB1*-
316 siRNA. Surprisingly, FOXB1-siRNA resulted in upregulation of NC marker expression
317 at day 5 as indicated by increased transcription of NC markers including *SOX10* (Fig 4E)
318 and proportion of SOX10⁺ cells (Fig. 4F). We then took advantage of CRISPR/CAS9
319 technologies. To this end, we removed the sequence encoding the Forkhead DNA-
320 binding domain of FOXB1 using a pair of guide RNAs (dgRNA) (Fig. 4G). PCR
321 genotyping and Sanger sequencing revealed specific deletion of the 278-bp genomic
322 region containing the sequence encoding the FOXB1 DNA-binding domain (Fig. 4H and
323 data not shown). Analysis with Western blot confirmed the loss of FOXB1 protein in
324 differentiating *FOXB1-KO* cell lines (Fig. S4B). We then assessed possible effects during
325 NC formation in KO lines and isogenic controls. Cultures from the parent human ES cell
326 line, 3 isogenic and 3 KO cell lines were processed for RT-qPCR analysis at ES cell
327 stage, day 3, and day 5. Confirming siRNA data, expression of neural border and NC
328 genes *PAX3*, *TFAP2A*, and *CHD6* were significantly upregulated at day 5 in KO over
329 control lines (Fig. 4I). Increases in expression for these genes however were already
330 observed at day 3, suggesting that loss of FOXB1 affected the early phase of NC
331 induction. Consistent with qPCR data, immunostaining of dgRNA-KO cells at day 5 also
332 revealed increased SOX10⁺ cells (data not shown). To confirm the dgRNA experiment,
333 we designed another experiment that targeted the translational start site of FOXB1 using
334 a single guide RNA (sgRNA) (Fig. S4D). We established a knockout (sgRNA-KO) and a
335 heterozygote (sgRNA-Het) cell line for analysis. We characterized the mutations in these
336 2 cell lines by TA-cloning (Fig. S4E) and verified the absence of FOXB1 protein in
337 sgRNA-KO line by western blotting (Fig. S4F). To provide a broader perspective of the
338 influence of FOXB1 in NC development we performed RNA-seq on these samples.
339 Principal component analysis of sgRNA-KO and sgRNA-Het transcriptome data of
340 differentiating cells collected at day 3 and day 5 revealed clear segregation of the

341 isogenic control, sgRNA-Het and sgRNA-KO cell lines according to their differentiation
342 time points by PC1, as well as tight correlations according to their genotypes at PC2,
343 revealing a potential dosage effect of FOXB1 function (Fig. S4G). Similar to dgRNA-KO
344 cell lines, we found that neural border and NC transcripts were upregulated in sgRNA-
345 Het and sgRNA-KO at both day 3 and day 5 (asterisks, Fig. S4H, table S4). A few pB
346 candidates were also upregulated (*DMBX1*, *OLFM3*, *PAX2*, *PKNOX2*) or downregulated
347 (*NRTK2*, *SOX21*, *VGLL3*) indicating that FOXB1 might feedback control selected pB
348 genes (double asterisks, Fig. S4H). Intriguingly, we also observed activation of
349 imprinting loci (*H19*, *IGF2*, *XIST*) (Fig. S4I), PRC2-regulated loci (*HOXA* and *HOXB*
350 clusters, as well as the neighboring homeodomain gene *EVX1*) (Fig. S4J and data not
351 shown), and loci related to increased cell proliferation (*EGFR*, *MYC*, and *S100A11*) (Fig.
352 S4K).

353 To investigate more precisely when does FOXB1 affects NC induction, we
354 performed time-series analyses (Fig. 4J). We found that dgRNA-KO cells underwent
355 accelerated NC induction, as revealed by a 24-hour earlier induction of neural border
356 genes *PAX3*, *PAX7*, and *TFAP2A* (Fig. 4K). Instead of an accelerated loss of pluripotency
357 marker expression as would be expected, expression dynamics for pluripotency gene
358 *POU5F1* appear similar in isogenic control and dgRNA-KO cells (Fig. 4L). Similarly,
359 expression of another pB gene *GBX2*, seem normal from day 1 to 3 in control and
360 dgRNA-KO cells (Fig. 4M). These results suggest that FOXB1 may regulate the temporal
361 acquisition of border specifiers and later NC markers, independently of *POU5F1*, and
362 *GBX2*. Then we interrogated if FOXB1 depletion modulates other fates. To this end we
363 deployed a BMP and Activin inhibitor cocktail on ES cell cultures to promote
364 neuroectoderm fate (Fig. 4N). Control and dgRNA-KO FOXB1 cells appear to attain
365 neuroectoderm precursor status and displayed no significant expression differences in
366 neuroectoderm markers *PAX6* and *HES5* (Fig. 4O), even though *HES5* dgRNA-KO
367 displayed a reduced transcription trend.

368 As indicated by comparable expression, loss of *FOXB1* also did not alter the
369 ability of dgRNA-KO cells line or sgRNA-KO cells to form mesoderm (T, Fig. 4P) or
370 definitive endoderm (*SOX17*, Fig. 4Q) (ES and ES-de, *EOMES*, *CER1*, and *SOX17*, Fig.
371 S4L, M) from ES cell stage, suggesting that FOXB1 effect on ES cell differentiation was

372 specific to NC lineage. These data altogether demonstrated that loss of FOXB1 promoted
373 the acquisition of NC.

374

375 FOXB1 Directly Regulated the Transcription of Key Neurogenic and Neural Crest Loci

376 To interrogate the molecular mechanism by which FOXB1 acted on the NC
377 differentiation program, we examined the genome-binding pattern of FOXB1. We
378 performed ChIP-seq of day 3 cultures when FOXB1 protein could be detected using a
379 specific anti-FOXB1 antibody (Fig. S4B, S4F). Peak calling against input sample
380 uncovered 3348 and 4388 high-confidence peaks for 2 wildtype ES cell samples
381 (FDR<0.1%, Day3WT1 and Day3WT2, Fig. 5A) that had significant overlaps with each
382 other (enrichment fold $\log_2=9.3$, $p<10^{-5}$, Fig 5A'), but only ~10 peaks each for 2 dgRNA-
383 KO samples (FDR<0.1%, Day3KO1 and Day3KO2, Fig. 5A). The 2158 day-3 common
384 peaks had enrichment of GC-rich repeats and forkhead transcription factor-binding motif
385 (data not shown and Fig. 5A''), and were specifically bound by FOXB1 as shown by heat
386 maps of aggregating ChIP-seq signals for wild type, dgRNA-KO, and input samples (Fig.
387 5B). Specificity of FOXB1 binding was additionally verified by ChIP-qPCR assay
388 against IgG and dgRNA-KO controls at selected FOXB1 bound regions (n=13, Fig.
389 S5A).

390 Volcano plot analysis of direct FOXB1 targets combining our above FOXB1
391 sgRNA-KO RNA-seq data and the FOXB1 CHIP-seq data set revealed 3 classes of gene
392 targets (Fig. 5C, Table S5). The first class included neural progenitor genes that were
393 downregulated (>2-fold in RPKM) in the FOXB1 sgRNA-KO day 3 transcriptome such
394 as *ASCL1*, *CRB2*, *RGMA* and *SOX1* (bolded, Fig. 5C). Of interest, *CRB2* and *SOX1* were
395 also identified as pB candidates (Fig. 1F'). The second class included FOXB1 direct
396 targets whose transcription were not affected in FOXB1 sgRNA-KO cells at day 3.
397 Among them, there were genes whose expression was normally increased in our
398 differentiating cultures such as *IGF1R* and *JAG1* (Fig. S1B), and several pB candidates
399 *BOC*, *CNTFR*, *GBX2*, *GREB1L*, *MAP2*, *MEIS2*, *OTX1* and *ZNF503* (Fig. 1F'). Neural
400 progenitor and differentiation genes (*FEZF2*, *ISL1*, *MSI1*, *POU6F1*), placodal ectoderm
401 regulator (*SIX1*), and general DNA methylation machinery components (*DNMT1* and
402 *DNMT3A*) were among FOXB1 targets whose expression was not affected at day 3

403 (Table S4). Lastly, the third class included upregulated genes (>2-fold in RPKM) such as
404 *BDNF*, *CCL2*, *COL1A2*, *DMBX1*, *HHIP*, *LINC01405*, *MSX2*, *PAPPA*, *PAX7*, *FAT1*,
405 *SALL3*, *TFAP2B*, and *TLE4* (bolded, Fig. 5C). Among the upregulated gene loci, some of
406 them were known NC genes such as *EDN1*, *MSX2*, *PAX7*, and *TFAP2B*, whereas others
407 were pB candidates (*DMBX1*, Fig 1F') or normally upregulated during NC induction
408 including *CCL2*, *COL1A2*, *FAT1*, *HHIP*, *PAPPA*, and *TLE4* (Fig. S1B and table S1).

409 By visualizing FOXB1-binding sites within target gene loci, we found that for
410 neural progenitor gene loci, FOXB1-binding sites could be found upstream of *ASCLI*,
411 *SOX1*, and *MSII* genes (asterisks, Fig. 6A-C). Among the FOXB1-bound elements in the
412 upregulated NC gene loci, some were intronic or located within gene bodies (*PAPPA*,
413 *PAX7*, *SALL3*, *TLE4*, *FAT1*, *HHIP*, and *TFAP2B* loci)(asterisks, Fig. 6D, E, S6A); others
414 were located either upstream (*BDNF*, *CCL2*, *COL1A2*, and *EDN1* loci) (asterisks, Fig.
415 6F, S6B) or downstream (asterisks, *MSX2* locus) (Fig. 6G).

416 Genome annotation revealed a significant proportion of intronic FOXB1-bound
417 elements and an enrichment of FOXB1-bound elements locating within promoters (9.6%)
418 and upstream regions (14.8%) (Fig. 6H). We found that many FOXB1-bound elements
419 within 5' UTR exons and promoters were either close to (Fig. 6A-B) or contained (Fig.
420 6C) CpG islands. We performed gene ontology analysis on a shortlisted FOXB1-bound
421 element set containing only 5' UTR exons, promoters and upstream elements (n=545).
422 We found significant enrichment of FOXB1 direct targets with gene sets correlated to
423 mammalian-specific phenotype, neuronal differentiation, and developmental processes
424 (Theiler stages 13 to 21) at peripheral (NC-derived) and central (neuroectoderm-derived)
425 nervous system structures (Fig. 6J) consistent with the model that FOXB1 directly
426 regulate human NC cell differentiation. In conclusion, our CHIP-seq data confirmed that
427 FOXB1 directly regulate NC gene induction by directly binding to NC and related gene
428 loci.

429

430 Loss of FOXB1 Function Leads to Long-term Suppression of Autonomic Neuronal Gene 431 Expression

432 Transient expression of a transcription factor can confer developmental
433 competence to differentiating cells to generate subsequent lineages as has been

434 demonstrated for other transcription factors such as Neurod1 (Pataskar et al., 2016) and
435 Foxa1/2 (Wang et al., 2015). The binding of FOXB1 in day 3 pre-NC cells to neural
436 progenitor gene loci could therefore carry such developmental function. One of these
437 neural progenitor loci, *ASCL1*, its gene product is a master regulator for neurogenic
438 potential as well as autonomic neuron differentiation (Lo et al., 1998; Oh et al., 2016).
439 NC contributes to mesenchymal progenitors and peripheral neurons including sensory
440 and autonomic neurons. We therefore speculated that removal of FOXB1, which directly
441 regulated *ASCL1*, would have a far-reaching effect on the differentiation program of
442 human NC cells towards autonomic lineages. While we also hypothesize that effect on
443 *ASCL1* expression or other direct targets may affect the balance of mesenchymal and
444 other neurogenic potentials in FOXB1 KO cell lines.

445 To test these hypotheses, we performed differentiation assay of day 5 isogenic
446 wildtype and dgRNA-KO cells (Fig. 7A) using a tri-inhibitor cocktail (CHIR 99021,
447 SU5402 and DAPT) to promote peripheral neuron (PN) formation (Chambers et al.,
448 2012; Leung et al., 2016), or FGF2 ligand to promote mesenchymal progenitor (MP)
449 formation (Fig. S7A-B). We observed that autonomic neuronal markers *ASCL1* (Fig. 7B),
450 *PHOX2A* (Fig. 7C), and *TH* (Fig. 7D), sensory neuron marker *POU4F1* (Fig. 7E) and
451 general neuronal marker *TUBB3* (Fig. 7F) were induced in day 11 isogenic control cells
452 under PN, but not under MP, condition, confirming that PN condition promotes both
453 sensory and autonomic neuron generation. Notably, *ASCL1* (Fig. 7B) and its downstream
454 targets in autonomic neuron development, the homeodomain transcription factor
455 (*PHOX2A*)(Fig. 7C), and the enzyme synthesizing the neurotransmitter noradrenaline
456 (*TH*) (Fig. 7D), were either not induced to the same extent as isogenic control cells or not
457 induced at all in dgRNA-KO under PN differentiation condition. Expression of general or
458 sensory peripheral neuron markers, such as *POU4F1* (Fig. 7E) and *TUBB3* (Fig. 7F),
459 however, were not changed in dgRNA-KO cells. Intriguingly, we observed that
460 mesenchymal markers *TWIST1* (Fig.7G) and *NT5E* (Fig.7H) were upregulated in day 5
461 and/or day 11-MP dgRNA-KO cells upon MP induction.

462 These data suggested that loss of FOXB1 function promoted expression of
463 mesenchymal genes but had a long-lasting effect on *ASCL1* gene transcription and might

464 therefore affect the ability of mature NC to generate autonomic neuronal progenitors as
465 indicated by inability of FOXB1 KO to upregulate other autonomic markers.

466 DISCUSSION

467 Identification and characterization of novel cell intermediates, especially those
468 that exist transiently in early embryos, is a challenging process. Here, we present a
469 pipeline for such research, which utilizes a range of techniques including time-course
470 transcriptomic analysis to identify key transcripts, signaling pathway perturbations to
471 characterize signal dependency, knockout of enhancers to demonstrate regulatory
472 functions, gene targeting of candidate factors and differentiation assays for phenotypic
473 characterization, and genome-wide chromatin binding data to pinpoint genomic
474 occupancy and to infer direct regulations and genetic networks. This pipeline could be
475 applied to studies of other cell types in stem cell and regenerative biology to identify
476 novel cellular states and intermediates. Our data here supports the existence of pB state,
477 however more definitive answers awaits further evidence, perhaps from the use of
478 approaches such as single cell RNA-sequencing and lineage tracing experiments would
479 provide more definitive proof. In this study, we also provide valuable resources and
480 genomic data sets for FOXB1 binding, β -catenin immediate targets during ES cell
481 differentiation, putative novel enhancer location for pB candidates/ β -catenin and
482 pluripotent factor regulated loci, as well as transcriptome of NC induction for data mining
483 and for generation of further testable hypotheses.

484 Our pioneer discovery of pB as a cellular intermediate during NC induction
485 (Leung et al., 2016) is gaining momentum and increasing attention in recent years in
486 embryo and reprogramming studies. For instance, a recent work describes a novel
487 population of ‘neural border stem cells’ reprogrammed from blood cells that bear
488 potential to generate central nervous system and NC derivatives (Thier et al., 2019). In
489 another study, Trevers et al., identifies embryonic ‘pB’ cells from pre-gastrula avian
490 embryos that bear resembling molecular signatures and differentiation potentials to our *in*
491 *vitro*-derived pB cells (Trevers et al., 2018). Our current manuscript serves as a follow-up
492 study for our previous work and others, and provides the molecular framework to derive
493 pB-like cells from embryos and other differentiated cell types for developmental, stem
494 cell, and therapeutic studies.

495 While inhibition of bone morphogenetic protein (BMP) signaling abolished
496 human NC induction and neural border gene expression, expression of pB genes was

497 preserved (Leung et al., 2016). In our expanded list of 68 pB candidates, we also found
498 that in almost all candidates tested including FOXB1, induction of these genes were
499 immune to inhibition of BMP signaling (data not shown). Such difference in responses to
500 BMP signaling hints at a potential strategic function of pB candidates in NC
501 development.

502 Our data identifies FOXB1 as a key factor limiting NC induction. Here, we show
503 that FOXB1 is expressed transiently in human pre-NC cells before the specification of
504 NC. We additionally show that *Foxb1* expresses in chick embryos prior to the appearance
505 of the neural plate border. Lineage tracing in mouse embryos supports the notion that
506 *Foxb1* is expressed in pre-NC cells and there is no evidence to suggest that it is present in
507 mature NC cells or their derivatives.

508 Our findings from FOXB1 ChIP-seq and the phenotypic analyses of FOXB1 KO
509 cells suggest a broader function of FOXB1 in directly regulating NC development.
510 FOXB1 function however is distinct from FOXD3, a pluripotent stem cell and NC factor,
511 whose expression complements FOXB1 during NC induction, and acts as an activator for
512 NC development. The fact that the neural border gene *PAX7* is directly regulated by
513 FOXB1 strongly indicates that FOXB1 acts upstream and represses the development of
514 the neural border stage. Sequence conservation analysis by MultiZ (Emera et al., 2016)
515 reveals that our FOXB1-bound elements are less evolutionary-conserved. More than 5%
516 of these elements are originated from the human clade (compared to <1% in control
517 elements) and up to 25% are primate or younger sequences (data not shown). We
518 postulate that evolution of these young elements could regulate NC developmental
519 processes, thereby shaping species-specific features during human and primate evolution.
520 Indeed, we found strong primate-specific FOXB1 bound elements within key NC loci
521 such as *MSX2* (+41K), *EDN1* (-131K), and *NR2F1* (-91K), which could potentially
522 contribute to the discrepancy between our data and murine embryo data that shows no
523 alteration of border/NC markers such as *Pax3* and *Msx1* in *FOXB1* mutant mice
524 (Labosky et al., 1997).

525 It is assumed that NC cells retain neurogenic potential from neurectoderm
526 progenitors, which NC was believed to derive from. But, here and in our previous work
527 (Leung et al., 2016), we have shown that NC and neural lineages segregated from each

528 other before the appearance of definitive neuroectoderm. NC cells therefore have to
529 establish its neurogenic potential in a mechanism either shared with or independent of
530 pre-neuroectoderm progenitors. We found that FOXB1 KO cells acquired a heightened
531 differentiation potential to generate mesenchymal progenitors. This was accompanied by
532 a deficiency in their ability to specify autonomic neuronal fate. Such defect in
533 differentiation potential could be due to a change of axial identity in FOXB1 KO cells
534 (which show an upregulation of anterior *HOX* genes), as migrating NC populations from
535 different axial identity of the rhombomeres are known to differentially contribute to
536 autonomic neuronal lineages (Lumb et al., 2014). Our CHIP-seq data however shows that
537 FOXB1 is directly activating and maintaining the competency of NC cells to express
538 *ASCL1*, an autonomic neuron master regulator (Lo et al., 1998). FOXB1 may act via
539 maintaining the open chromatin structures at *ASCL1* proximal promoter and/or other
540 unknown epigenetic mechanisms to maintain NC cell competency to induce *ASCL1*
541 expression. On the other hand, it could act as a classic transcription factor via recruitment
542 of co-activators or co-repressors to activate or repress target gene expression similar to
543 other FOX family proteins (Lalmansingh et al., 2012), or specific domains within the
544 FOX factor could specify these distinct transcriptional activities as have previously
545 shown for other FOX factors (Neilson et al., 2012).

546 Interestingly, we also find that a significant portion of our FOXB1 peaks (>30%)
547 are occupied by the neuron subtype-specific transcription factor and an autism
548 susceptible gene FOXP1 in human neural progenitor cell lines (Araujo et al., 2015)(data
549 not shown) suggesting that FOXB1 may carry unknown functions in regulating latter
550 neural development.

551 The early requirement of WNT/ β -catenin signaling for human NC induction
552 (Leung et al., 2016; Menendez et al., 2011; Mica et al., 2013) has been reported in
553 vertebrate model organisms such as birds, amphibians and fish (Basch et al., 2006; Chang
554 and Hemmati-Brivanlou, 1998; Garcia-Castro et al., 2002; Patthey et al., 2009; Saint-
555 Jeannet et al., 1997)(Prasad et al., submitted). Our data supports a model in which
556 WNT/ β -catenin signaling directly activates a panel of pB genes including FOXB1 and
557 other factors such as GBX2 and SP5 that in turn regulate the specification, lineage
558 competency, and differentiation timing of differentiating ES cells to acquire NC fate.

559 Previous works have demonstrated pre-border genes GBX2 and SP5 acting upstream of
560 neural border genes to induce the latter expression (Li et al., 2009; Park et al., 2013). We
561 propose that pro-neural crest factors such as GBX2 and SP5 could act parallel to FOXB1
562 to influence NC fate choice.

563 This work further suggest that the proposed transient pB cell stage has unique
564 transcriptional, epigenetic and functional features, different from the pluripotent cell state
565 from which it emerges, and from later stages NC progenitors found at the neural plate
566 border and neural folds. We have confirmed early expression for several pB gene
567 candidates prior to expression of neural plate border genes in chick embryos, and
568 demonstrated in our human system their early expression to be canonical WNT
569 dependent and insensitive to BMP inhibition. Focusing on FOXB1 as a pB gene example,
570 we showed that it directly regulates NC loci, temporally controls progression of
571 differentiating cells towards more advanced NC state, and carries a remarkable impact in
572 terminal differentiation driven by its early transient expression. These findings lend
573 strong support to our proposed pB state and its significance to NC ontogeny.

574

575 ACKNOWLEDGEMENTS

576 We thank Dr. Caihong Qiu, Yinghong Ma, and Jason Thomsen at the Yale Stem Cell
577 Core for providing access to core facility and human pluripotent stem cell lines, and Dr.
578 Kaya Bilguvar, Christopher Castaldi, and Bryan Pasqualucci at the Yale Center for
579 Genome Analysis (YCGA) and Dr. Mei Zhang at the Genomics and Bioinformatics Core
580 for high throughput sequencing services. We thank Dr. James Noonan for his critical
581 advice on the design of the FOXB1 ChIP-seq experiment. We also thank Dr. Giuseppe
582 Amatulli and Dr. Dejian Zhan for providing assistance on bioinformatics analysis. All
583 public data sets were downloaded from Cistrome database. This work is supported by
584 funding from Connecticut Innovations and NIH R01DE017914.

585 AUTHOR CONTRIBUTIONS

586 Conceptualization: A.W.L., A.Z.X., M.I.G.C.; Methodology: A.W.L., C.B.; Software:
587 F.L-G; Writing - Original Draft: A.W.L.; Writing – Review & Editing: A.W.L., A.Z.X.,
588 M.I.G.C; Formal analysis: A.W.L., F.L-G; Investigation: A.W.L., B.C., M.S.P., J.C.;
589 Visualization: A.W.L., F.L-G, K.L.; Funding acquisition: A.Z.X., M.I.G.C.
590

591 DECLARATION OF INTERESTS

592 The authors declare no conflict of interests.

593 REFERENCE

- 594 Alvarez-Bolado, G., Zhou, X., Voss, A.K., Thomas, T., and Gruss, P. (2000). Winged
595 helix transcription factor Foxb1 is essential for access of mammillothalamic axons to
596 the thalamus. *Development (Cambridge, England)* 127, 1029-1038.
- 597 Araujo, D.J., Anderson, A.G., Berto, S., Runnels, W., Harper, M., Ammanuel, S., Rieger,
598 M.A., Huang, H.C., Rajkovich, K., Loerwald, K.W., *et al.* (2015). FoxP1 orchestration of
599 ASD-relevant signaling pathways in the striatum. *Genes & development* 29, 2081-
600 2096.
- 601 Arduini, B.L., and Brivanlou, A.H. (2012). Modulation of FOXD3 activity in human
602 embryonic stem cells directs pluripotency and paraxial mesoderm fates. *Stem cells*
603 30, 2188-2198.
- 604 Basch, M.L., Bronner-Fraser, M., and Garcia-Castro, M.I. (2006). Specification of the
605 neural crest occurs during gastrulation and requires Pax7. *Nature* 441, 218-222.
- 606 Betschinger, J., Nichols, J., Dietmann, S., Corrin, P.D., Paddison, P.J., and Smith, A.
607 (2013). Exit from pluripotency is gated by intracellular redistribution of the bHLH
608 transcription factor Tfe3. *Cell* 153, 335-347.
- 609 Betters, E., Charney, R.M., and Garcia-Castro, M.I. (2018). Early specification and
610 development of rabbit neural crest cells. *Dev Biol*.
- 611 Chambers, S.M., Qi, Y., Mica, Y., Lee, G., Zhang, X.J., Niu, L., Bilslund, J., Cao, L., Stevens,
612 E., Whiting, P., *et al.* (2012). Combined small-molecule inhibition accelerates
613 developmental timing and converts human pluripotent stem cells into nociceptors.
614 *Nature biotechnology* 30, 715-720.
- 615 Chang, C., and Hemmati-Brivanlou, A. (1998). Neural crest induction by Xwnt7B in
616 *Xenopus*. *Dev Biol* 194, 129-134.
- 617 Consortium, E.P. (2012). An integrated encyclopedia of DNA elements in the human
618 genome. *Nature* 489, 57-74.
- 619 Emera, D., Yin, J., Reilly, S.K., Gockley, J., and Noonan, J.P. (2016). Origin and
620 evolution of developmental enhancers in the mammalian neocortex. *Proceedings of*
621 *the National Academy of Sciences of the United States of America* 113, E2617-2626.
- 622 Estaras, C., Benner, C., and Jones, K.A. (2015). SMADs and YAP compete to control
623 elongation of beta-catenin:LEF-1-recruited RNAPII during hESC differentiation.
624 *Molecular cell* 58, 780-793.
- 625 Fernandez-Garre, P., Rodriguez-Gallardo, L., Gallego-Diaz, V., Alvarez, I.S., and
626 Puellas, L. (2002). Fate map of the chicken neural plate at stage 4. *Development*
627 (Cambridge, England) 129, 2807-2822.
- 628 Funa, N.S., Schachter, K.A., Lerdrup, M., Ekberg, J., Hess, K., Dietrich, N., Honore, C.,
629 Hansen, K., and Semb, H. (2015). beta-Catenin Regulates Primitive Streak Induction
630 through Collaborative Interactions with SMAD2/SMAD3 and OCT4. *Cell Stem Cell*
631 16, 639-652.
- 632 Garcia-Castro, M.I., Marcelle, C., and Bronner-Fraser, M. (2002). Ectodermal Wnt
633 function as a neural crest inducer. *Science* 297, 848-851.
- 634 Genga, R.M.J., Kernfeld, E.M., Parsi, K.M., Parsons, T.J., Ziller, M.J., and Maehr, R.
635 (2019). Single-Cell RNA-Sequencing-Based CRISPRi Screening Resolves Molecular
636 Drivers of Early Human Endoderm Development. *Cell Rep* 27, 708-718 e710.

637 Gertz, J., Savic, D., Varley, K.E., Partridge, E.C., Safi, A., Jain, P., Cooper, G.M., Reddy,
638 T.E., Crawford, G.E., and Myers, R.M. (2013). Distinct properties of cell-type-specific
639 and shared transcription factor binding sites. *Molecular cell* 52, 25-36.

640 Golson, M.L., and Kaestner, K.H. (2016). Fox transcription factors: from development
641 to disease. *Development (Cambridge, England)* 143, 4558-4570.

642 Hackett, J.A., Huang, Y., Gunesdogan, U., Gretarsson, K.A., Kobayashi, T., and Surani,
643 M.A. (2018). Tracing the transitions from pluripotency to germ cell fate with CRISPR
644 screening. *Nature communications* 9, 4292.

645 Hall, B.K. (2000). The neural crest as a fourth germ layer and vertebrates as
646 quadroblastic not triploblastic. *Evolution & development* 2, 3-5.

647 Iwafuchi-Doi, M., and Zaret, K.S. (2016). Cell fate control by pioneer transcription
648 factors. *Development (Cambridge, England)* 143, 1833-1837.

649 Kalkan, T., and Smith, A. (2014). Mapping the route from naive pluripotency to
650 lineage specification. *Philosophical transactions of the Royal Society of London*
651 *Series B, Biological sciences* 369.

652 Kos, R., Reedy, M.V., Johnson, R.L., and Erickson, C.A. (2001). The winged-helix
653 transcription factor FoxD3 is important for establishing the neural crest lineage and
654 repressing melanogenesis in avian embryos. *Development (Cambridge, England)*
655 *128*, 1467-1479.

656 Krishnakumar, R., Chen, A.F., Pantovich, M.G., Danial, M., Parchem, R.J., Labosky, P.A.,
657 and Bllloch, R. (2016). FOXD3 Regulates Pluripotent Stem Cell Potential by
658 Simultaneously Initiating and Repressing Enhancer Activity. *Cell stem cell* 18, 104-
659 117.

660 Labosky, P.A., Winnier, G.E., Jetton, T.L., Hargett, L., Ryan, A.K., Rosenfeld, M.G.,
661 Parlow, A.F., and Hogan, B.L. (1997). The winged helix gene, Mf3, is required for
662 normal development of the diencephalon and midbrain, postnatal growth and the
663 milk-ejection reflex. *Development (Cambridge, England)* 124, 1263-1274.

664 Lalmansingh, A.S., Karmakar, S., Jin, Y., and Nagaich, A.K. (2012). Multiple modes of
665 chromatin remodeling by Forkhead box proteins. *Biochim Biophys Acta* 1819, 707-
666 715.

667 Leung, A.W., Murdoch, B., Salem, A.F., Prasad, M.S., Gomez, G.A., and Garcia-Castro,
668 M.I. (2016). WNT/beta-catenin signaling mediates human neural crest induction via
669 a pre-neural border intermediate. *Development* 143, 398-410.

670 Li, B., Kuriyama, S., Moreno, M., and Mayor, R. (2009). The posteriorizing gene Gbx2
671 is a direct target of Wnt signalling and the earliest factor in neural crest induction.
672 *Development (Cambridge, England)* 136, 3267-3278.

673 Lo, L., Tiveron, M.C., and Anderson, D.J. (1998). MASH1 activates expression of the
674 paired homeodomain transcription factor Phox2a, and couples pan-neuronal and
675 subtype-specific components of autonomic neuronal identity. *Development*
676 *(Cambridge, England)* 125, 609-620.

677 Lukoseviciute, M., Gavriouchkina, D., Williams, R.M., Hochgreb-Hagele, T.,
678 Senanayake, U., Chong-Morrison, V., Thongjuea, S., Repapi, E., Mead, A., and Sauka-
679 Spengler, T. (2018). From Pioneer to Repressor: Bimodal foxd3 Activity Dynamically
680 Remodels Neural Crest Regulatory Landscape In Vivo. *Dev Cell* 47, 608-628 e606.

681 Lumb, R., Wiszniak, S., Kabbara, S., Scherer, M., Harvey, N., and Schwarz, Q. (2014).
682 Neuropilins define distinct populations of neural crest cells. *Neural development* 9,
683 24.
684 Ma, Y., Yao, N., Liu, G., Dong, L., Liu, Y., Zhang, M., Wang, F., Wang, B., Wei, X., Dong, H.,
685 *et al.* (2015). Functional screen reveals essential roles of miR-27a/24 in
686 differentiation of embryonic stem cells. *The EMBO journal* 34, 361-378.
687 Menendez, L., Yatskievych, T.A., Antin, P.B., and Dalton, S. (2011). Wnt signaling and
688 a Smad pathway blockade direct the differentiation of human pluripotent stem cells
689 to multipotent neural crest cells. *Proc Natl Acad Sci U S A* 108, 19240-19245.
690 Mica, Y., Lee, G., Chambers, S.M., Tomishima, M.J., and Studer, L. (2013). Modeling
691 neural crest induction, melanocyte specification, and disease-related pigmentation
692 defects in hESCs and patient-specific iPSCs. *Cell Rep* 3, 1140-1152.
693 Neilson, K.M., Klein, S.L., Mhaske, P., Mood, K., Daar, I.O., and Moody, S.A. (2012).
694 Specific domains of FoxD4/5 activate and repress neural transcription factor genes
695 to control the progression of immature neural ectoderm to differentiating neural
696 plate. *Dev Biol* 365, 363-375.
697 Oh, Y., Cho, G.S., Li, Z., Hong, I., Zhu, R., Kim, M.J., Kim, Y.J., Tampakakis, E., Tung, L.,
698 Haganir, R., *et al.* (2016). Functional Coupling with Cardiac Muscle Promotes
699 Maturation of hPSC-Derived Sympathetic Neurons. *Cell stem cell* 19, 95-106.
700 Park, D.S., Seo, J.H., Hong, M., Bang, W., Han, J.K., and Choi, S.C. (2013). Role of Sp5 as
701 an essential early regulator of neural crest specification in xenopus. *Developmental*
702 *dynamics : an official publication of the American Association of Anatomists* 242,
703 1382-1394.
704 Pataskar, A., Jung, J., Smialowski, P., Noack, F., Calegari, F., Straub, T., and Tiwari, V.K.
705 (2016). NeuroD1 reprograms chromatin and transcription factor landscapes to
706 induce the neuronal program. *The EMBO journal* 35, 24-45.
707 Patthey, C., Edlund, T., and Gunhaga, L. (2009). Wnt-regulated temporal control of
708 BMP exposure directs the choice between neural plate border and epidermal fate.
709 *Development (Cambridge, England)* 136, 73-83.
710 Pijuan-Sala, B., Guibentif, C., and Gottgens, B. (2018). Single-cell transcriptional
711 profiling: a window into embryonic cell-type specification. *Nat Rev Mol Cell Biol* 19,
712 399-412.
713 Prasad, M.S., Charney, R.M., and Garcia-Castro, M.I. (2019). Specification and
714 formation of the neural crest: Perspectives on lineage segregation. *Genesis* 57,
715 e23276.
716 Rada-Iglesias, A., Bajpai, R., Swigut, T., Brugmann, S.A., Flynn, R.A., and Wysocka, J.
717 (2011). A unique chromatin signature uncovers early developmental enhancers in
718 humans. *Nature* 470, 279-283.
719 Respuela, P., Nikolic, M., Tan, M., Frommolt, P., Zhao, Y., Wysocka, J., and Rada-
720 Iglesias, A. (2016). Foxd3 Promotes Exit from Naive Pluripotency through Enhancer
721 Decommissioning and Inhibits Germline Specification. *Cell stem cell* 18, 118-133.
722 Saint-Jeannet, J.P., He, X., Varmus, H.E., and Dawid, I.B. (1997). Regulation of dorsal
723 fate in the neuraxis by Wnt-1 and Wnt-3a. *Proceedings of the National Academy of*
724 *Sciences of the United States of America* 94, 13713-13718.

725 Sasai, N., Mizuseki, K., and Sasai, Y. (2001). Requirement of FoxD3-class signaling for
726 neural crest determination in *Xenopus*. *Development (Cambridge, England)* *128*,
727 2525-2536.

728 Seo, S., Chen, L., Liu, W., Zhao, D., Schultz, K.M., Sasman, A., Liu, T., Zhang, H.F., Gage,
729 P.J., and Kume, T. (2017). *Foxc1* and *Foxc2* in the Neural Crest Are Required for
730 Ocular Anterior Segment Development. *Investigative ophthalmology & visual
731 science* *58*, 1368-1377.

732 Seo, S., and Kume, T. (2006). Forkhead transcription factors, *Foxc1* and *Foxc2*, are
733 required for the morphogenesis of the cardiac outflow tract. *Dev Biol* *296*, 421-436.

734 Stuhlmiller, T.J., and Garcia-Castro, M.I. (2012). Current perspectives of the signaling
735 pathways directing neural crest induction. *Cell Mol Life Sci* *69*, 3715-3737.

736 Takebayashi-Suzuki, K., Kitayama, A., Terasaka-Iioka, C., Ueno, N., and Suzuki, A.
737 (2011). The forkhead transcription factor *FoxB1* regulates the dorsal-ventral and
738 anterior-posterior patterning of the ectoderm during early *Xenopus* embryogenesis.
739 *Dev Biol* *360*, 11-29.

740 Teng, L., Mundell, N.A., Frist, A.Y., Wang, Q., and Labosky, P.A. (2008). Requirement
741 for *Foxd3* in the maintenance of neural crest progenitors. *Development (Cambridge,
742 England)* *135*, 1615-1624.

743 Teo, A.K., Arnold, S.J., Trotter, M.W., Brown, S., Ang, L.T., Chng, Z., Robertson, E.J.,
744 Dunn, N.R., and Vallier, L. (2011). Pluripotency factors regulate definitive endoderm
745 specification through *eomesodermin*. *Genes & development* *25*, 238-250.

746 Thier, M.C., Hommerding, O., Panten, J., Pinna, R., Garcia-Gonzalez, D., Berger, T.,
747 Worsdorfer, P., Assenov, Y., Scognamiglio, R., Przybylla, A., *et al.* (2019).
748 Identification of Embryonic Neural Plate Border Stem Cells and Their Generation by
749 Direct Reprogramming from Adult Human Blood Cells. *Cell stem cell* *24*, 166-182
750 e113.

751 Trevers, K.E., Prajapati, R.S., Hintze, M., Stower, M.J., Strobl, A.C., Tambalo, M.,
752 Ranganathan, R., Moncaut, N., Khan, M.A.F., Stern, C.D., *et al.* (2018). Neural
753 induction by the node and placode induction by head mesoderm share an initial
754 state resembling neural plate border and ES cells. *Proceedings of the National
755 Academy of Sciences of the United States of America* *115*, 355-360.

756 Tsankov, A.M., Gu, H., Akopian, V., Ziller, M.J., Donaghey, J., Amit, I., Gnirke, A., and
757 Meissner, A. (2015). Transcription factor binding dynamics during human ES cell
758 differentiation. *Nature* *518*, 344-349.

759 Wang, A., Yue, F., Li, Y., Xie, R., Harper, T., Patel, N.A., Muth, K., Palmer, J., Qiu, Y.,
760 Wang, J., *et al.* (2015). Epigenetic priming of enhancers predicts developmental
761 competence of hESC-derived endodermal lineage intermediates. *Cell stem cell* *16*,
762 386-399.

763 Wang, Z., Oron, E., Nelson, B., Razis, S., and Ivanova, N. (2012). Distinct lineage
764 specification roles for *NANOG*, *OCT4*, and *SOX2* in human embryonic stem cells. *Cell
765 stem cell* *10*, 440-454.

766 Wehr, R., Mansouri, A., de Maeyer, T., and Gruss, P. (1997). *Fkh5*-deficient mice show
767 dysgenesis in the caudal midbrain and hypothalamic mammillary body.
768 *Development (Cambridge, England)* *124*, 4447-4456.

769 Xu, P., Balczerski, B., Ciozda, A., Louie, K., Oralova, V., Huysseune, A., and Crump, J.G.
770 (2018). Fox proteins are modular competency factors for facial cartilage and tooth
771 specification. *Development (Cambridge, England)* 145.
772 Yamamoto, T., Mencarelli, M.A., Di Marco, C., Mucciolo, M., Vascotto, M., Balestri, P.,
773 Gerard, M., Mathieu-Dramard, M., Andrieux, J., Breuning, M., *et al.* (2014).
774 Overlapping microdeletions involving 15q22.2 narrow the critical region for
775 intellectual disability to NARG2 and RORA. *Eur J Med Genet* 57, 163-168.
776 Zhao, T., Zhou, X., Szabo, N., Leitges, M., and Alvarez-Bolado, G. (2007). Foxb1-driven
777 Cre expression in somites and the neuroepithelium of diencephalon, brainstem, and
778 spinal cord. *Genesis* 45, 781-787.
779

780 FIGURE LEGENDS

781 **Figure 1.** Identification of pre-border candidates by transcriptomic analysis. (A)
782 Schematic diagram depicting the differentiation program for human NC induction.
783 Asterisks indicate time points when samples were harvested for RNA-seq. (B) SOX10
784 and PAX6 immunostaining of day 5 NC cells. (C) Hierarchical clustering of all expressed
785 genes from ESC, day 3 and day 5 transcriptomes. (D, E) K-means clustering of the
786 RPKM values of transcripts mapped in the ESC, day 3 and day 5 transcriptomes that are
787 functionally associated with pluripotency and self renewal of human ES cells (D), or
788 neural plate border, pre-migratory neural crest and differentiating neural crest cells (E).
789 Relative intensities were displayed with blue being lowest in expression level to red
790 being highest. (F) Plot of all transcripts identified from RNA-seq with day 3 RPKM
791 values plotted against day 3 fold change over day 0 (ES cells) (F') Pink boxed-region is
792 magnified on the right to display the 68 pB candidates transcripts. The 4 pre-border
793 candidates identified in (Leung et al., 2016) are displayed in bold.

794

795 **Figure 2.** β -catenin positively regulates pB candidate gene induction. (A) Schematic
796 diagram showing lentiviral constructs containing luciferase and β -catenin shRNAs and
797 the procedures for generating stably infected shRNA expressing human ES cell lines. (B)
798 qPCR data of *CTNNB1* and *POU5F1* comparing control (luciferase shRNA) against
799 knockdown (β -catenin shRNA) in ES and day 1 cultures. (C) Heat map of the expression
800 dynamics of the 68 pB candidates in control and knockdown cell lines derived from
801 RNA-seq data of ES cell, day 1 and day 3 cells generated using Morpheus. (D)
802 Differentiation day 3 cultures treated with or without FGF2 ligand at the indicated
803 concentration. Dunnett's multiple comparison tests were carried to calculate statistics
804 between control group with ligand-treated groups. (E) Differentiation day 3 cultures
805 treated with or without BMP4 ligand. Fisher's LSD test was used. (F) A step-wise
806 induction model for human NC and a gene regulatory network of human NC with
807 signaling inputs from canonical WNT, FGF and BMP signaling.

808

809 **Figure 3.** Functional characterization of pB gene regulatory elements. (A-C) Loci for pB
810 candidate embedded with published ChIP-seq and ATAC-seq data sets in bigwig formats

811 were displayed on UCSC browsers. ‘ESC stage’ indicates the sequencing data were
812 derived from human ES cells. ‘WNT-Dif’ indicates the data were from human ES cells
813 treated with CHIR 99021 or WNT3A ligand. qPCR measurements on ChIP DNA pulled
814 down using anti-NANOG (D) and anti-H3K27ac (E) antibodies. Isotype-matched IgGs
815 were used as controls. Asterisks directly above standard deviation bars represent
816 comparisons between IgG and H3K27ac groups at their corresponding time points. One-
817 way ANOVA tests were carried out with Bonferroni’s corrections for multiple testing.
818 (F) CRISPR targeting strategy for FOXB1-E1 element. (G) PCR genotyping of isogenic
819 and FOXB1-E1 targeted clones. Expected sizes of wildtype and knockout PCR products
820 are shown on the right. (H) Day wise time course quantification of *FOXB1* expression
821 during NC induction in isogenic-WT1 and FOXB1-E1-KO1 cell lines. Three culture
822 samples were collected for each cell lines at each differentiation day. Unpaired t-tests
823 with Holm-Sidak corrections for multiple testing were carried out on the indicated time
824 points. (I) Normalized expression values and statistics at each time points were displayed.
825

826 **Figure 4.** Phenotypic characterization of a human *FOXB1* loss-of-function cell model.
827 (A) RNA-seq reads on human *FOXB1* locus converted to bigwig format and displayed on
828 igv software. Sample labeling refers to Fig 1C. (B) Time course-qPCR analysis of
829 selected FOX transcription factor transcripts during ES cell differentiation. (C-D) *Foxb1*
830 *in situ* hybridization in HH4 and HH8 stage chick embryos. Transverse sections are
831 displayed to the right (C’ and D’). Arrows are pointing to the ectoderm cell layer.
832 Asterisks indicate the position of the neural plate border. (E) qPCR data of NC factors on
833 day 5 cultures treated with control or FOXB1 siRNA. A representative of 3 biological
834 replicates is displayed. (F) DAPI staining and SOX10 immunostaining of day 5 cultures
835 treated with control or FOXB1 siRNA. Magnified images for SOX10+ cells are displayed
836 in the insets. (G) CRISPR targeting strategy for CRISPR-mediated mutations at the DNA
837 binding domain sequence of *FOXB1* gene using two gRNAs. (H) PCR genotyping of
838 isogenic and dgRNA targeted cell lines. (I) Time-course qPCR measurements of NC
839 factors on three isogenic and dgRNA-KO cell lines. Two-way ANOVA was performed
840 with Dunnett correction for multiple testing. (J) Differentiation and sample collection
841 schematics for NC induction. (K) Time-course qPCR data of NC genes for isogenic

842 wildtype and dgRNA-KO cell lines during NC induction. Multiple t-tests with Holm-
843 Sidak corrections were performed. (L, M). *POU5F1* and *GBX2* time-course qPCR
844 comparing isogenic control and *FOXB1* dgRNA-KO cell lines. Multiple t-tests with
845 Holm-Sidak corrections were performed. (N) Differentiation and sample collection
846 schematics for neurectoderm competency test. (O) Time-course qPCR data of
847 neurectoderm genes during differentiation using a schematic displayed in panel N.
848 Multiple t-tests with Holm-Sidak corrections were performed. Isogenic wildtype and
849 sgRNA-KO ES cells were treated with FGF2 or Activin to promote mesoderm (P) and
850 definitive endoderm (Q) induction as indicated by T and SOX17 immunostaining
851 respectively.

852

853 **Figure 5.** Global genomic binding analysis of FOXB1 protein during human neural crest
854 induction. (A) Peak numbers called from FOXB1 ChIP-seq on 2 wildtype and 2 dgRNA-
855 KO samples. (A') Venn diagram showing overlapping elements for the 2 wildtype ChIP-
856 seq samples. (A'') Motif analysis of 2158 FOXB1-bound elements. (B) Heat map of
857 signals centered on the 2158 FOXB1-bound elements for 2 wildtype, 2 knockout and an
858 input samples. (C) Volcano plot of all FOXB1 targets within a 50kb window from TSS.
859 Purple dots indicate genes that are differentially expressed in our earlier ES, day 3 and
860 day 5 transcriptome (Fig 1). Bolded genes are key candidates for neural and NC
861 development.

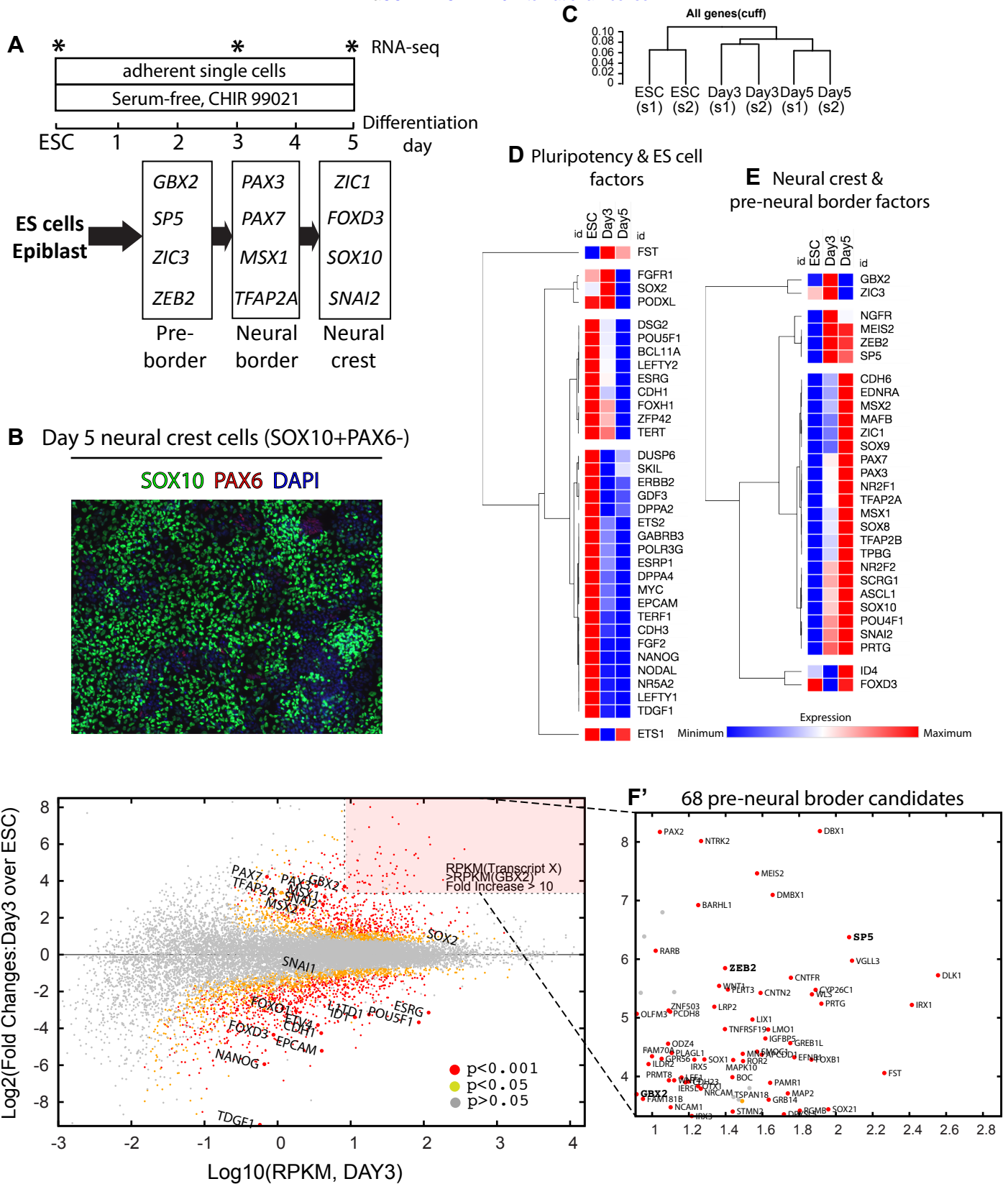
862

863 **Figure 6.** FOXB1 directly regulates target neural and neural crest genes. IGV tracks
864 displaying ChIP-seq signals for the 2 wildtype, 2 knockout samples, and an optional CpG
865 annotation at neuronal progenitor (A-C) and neural crest (D-G) gene loci. Asterisks
866 indicate location of called peaks. (H) Genome annotation of the 2158 common FOXB1
867 peak regions using NCBI Ref. Seq. build hg19. Priority was set as follows: Promoters,
868 5'UTR exons, upstream sequences, 3'UTR exons, coding exons, introns, downstream
869 sequences and intergenic regions. Actual peak numbers are shown in brackets. (I) The
870 545 selected FOXB1-bound elements, contained within upstream elements, promoters,
871 and 5' UTR exons, were further classified according to the presence or absence of CpG

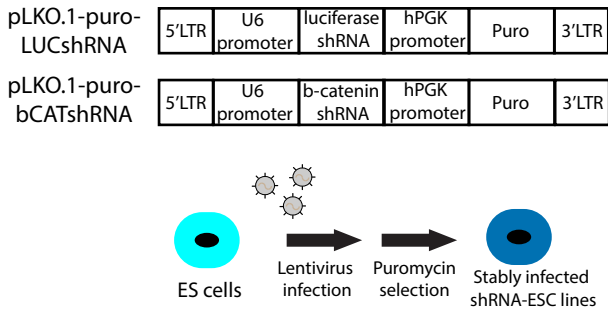
872 islands. (J) GREAT gene ontology analysis of the 545 selected FOXB1 peak set using a
873 20 kb genomic window.

874

875 **Figure 7.** *FOXB1* regulates autonomic neuron differentiation potential in NC cells. (A)
876 Terminal differentiation schematic for NC cells. qPCR analysis of autonomic neuronal
877 (B-D), sensory and general neuronal (E-F) and mesenchymal progenitor (G-H) markers
878 on ES, day 5 and differentiated day 11 isogenic control and dgRNA-KO cells.

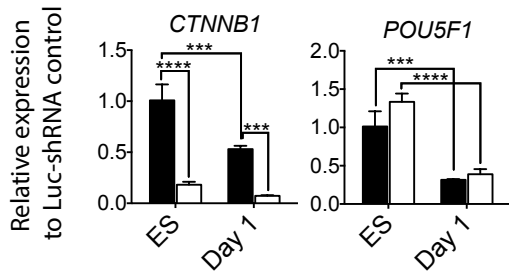


A

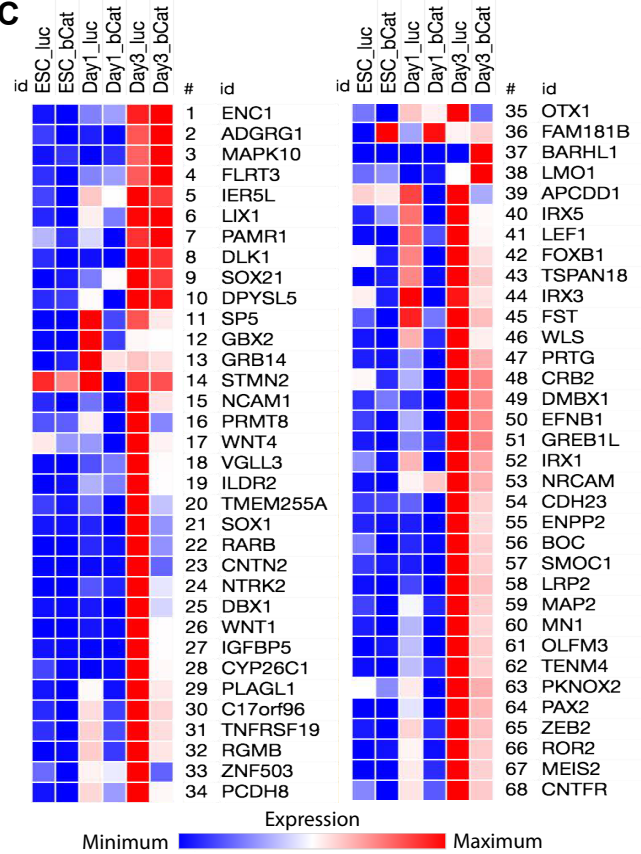


B ■ luciferase shRNA
□ β-catenin shRNA

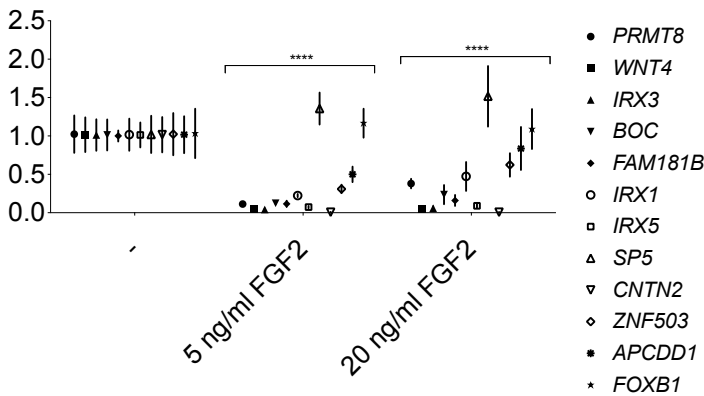
ES cells and differentiation day 1



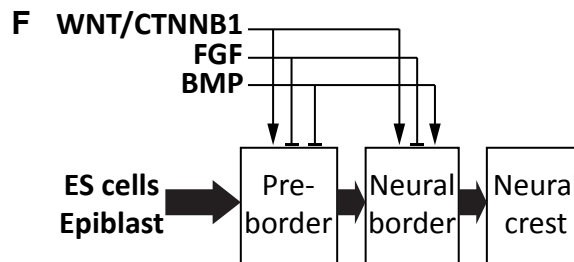
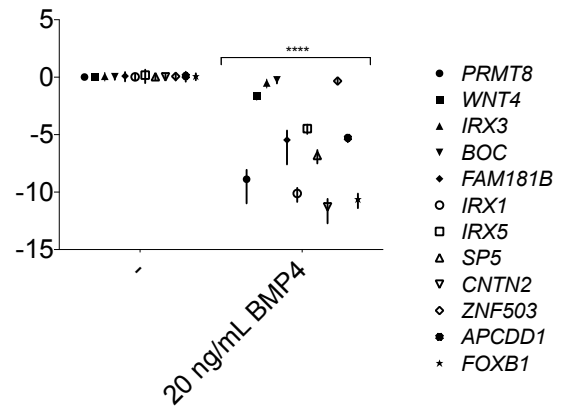
C



D

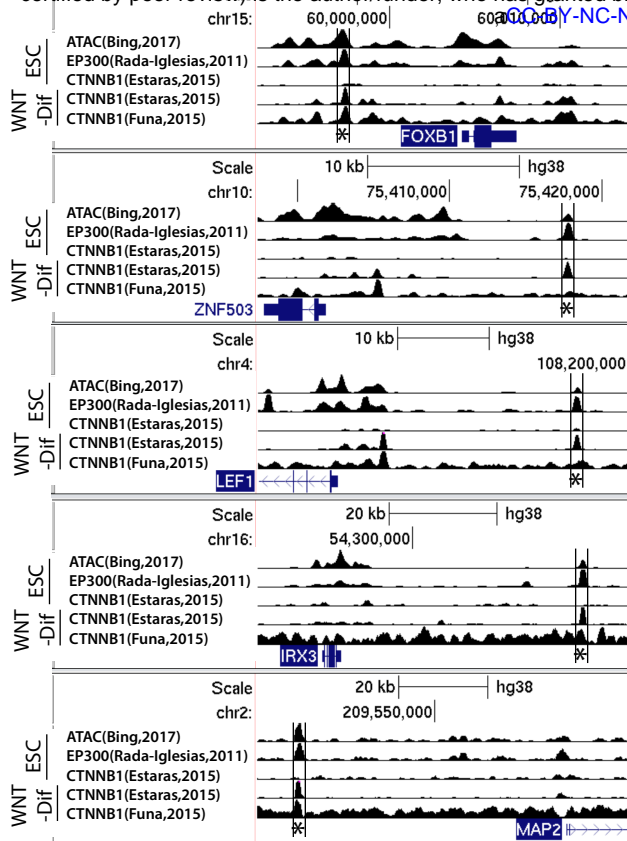


E

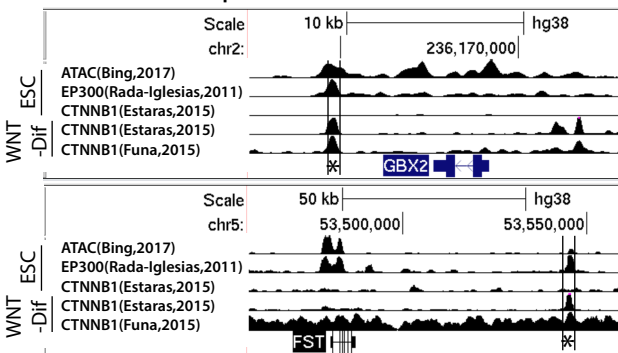


A Upstream pB enhancers

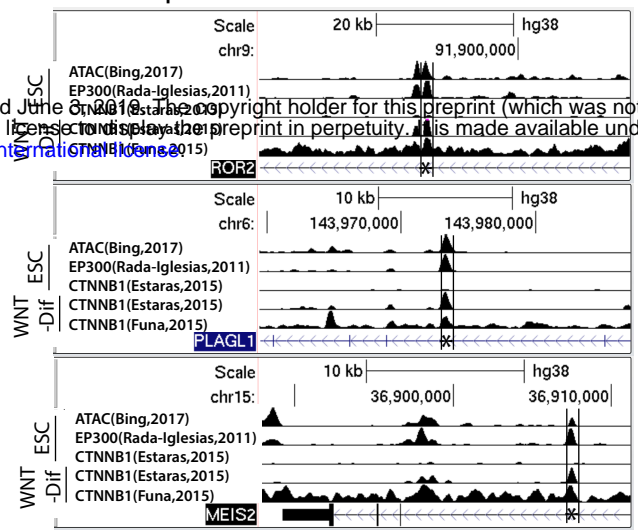
bioRxiv preprint doi: <https://doi.org/10.1101/646026>; this version posted June 3, 2019. The copyright holder for this preprint (which was not certified by peer review) is the author/funder, who has granted bioRxiv a license to display the preprint in perpetuity. It is made available under aCC-BY-NC-ND 4.0 International license.



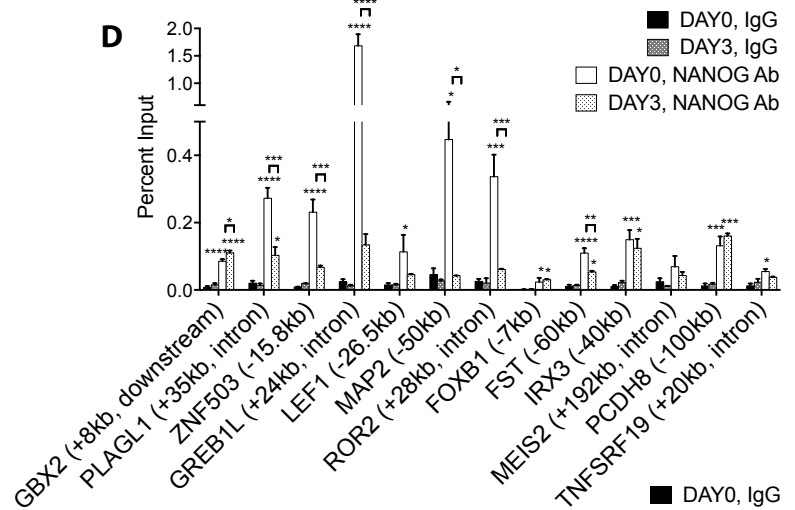
B Downstream pB enhancers



C Intronic pB enhancers



D



E

